Studies of Peptides Forming 3_{10}- and α-Helices and β-Bend Ribbon Structures in Organic Solution and in Model Biomembranes by Fourier Transform Infrared Spectroscopy†

D. F. Kennedy,‡ M. Crisma,§ C. Toniolo,§ and D. Chapman*,‡

Department of Protein and Molecular Biology, Division of Basic Medical Science, Royal Free Hospital School of Medicine, University of London, London NW3 2PF, United Kingdom, and Biopolymer Research Centre, CNR, Department of Organic Chemistry, University of Padua, 35131 Padua, Italy

Received November 20, 1990; Revised Manuscript Received March 20, 1991

ABSTRACT: In order to examine the potential correlation between infrared absorption spectra and 3_{10}- and α-helices and β-bend ribbon structures, the secondary structures of synthetic peptides known to contain pure 3_{10}-helices, mixed $3_{10}/\alpha$-helices, and pure β-bend ribbon structures, based upon X-ray diffraction and NMR studies, have been investigated by using FTIR spectroscopy incorporating resolution-enhancement techniques. Studies of the peptides known to contain a stable 3_{10}-helix in $CDCl_3$ show the main amide I band of fully stable 3_{10}-helices occurs at 1666–1662 cm^{-1}. Resolution-enhancement methods revealed small contributions at 1681–1678 and 1646–1644 cm^{-1}, while the amide II band occurs at 1533–1531 cm^{-1}. Peptides known to contain both α- and 3_{10}-helices in their structure exhibit bands characteristic of both types of conformation. Peptides known to fold into the β-bend ribbon structure show an amide I band maximum at 1648–1645 cm^{-1} with the amide II band at 1538–1536 cm^{-1}. Incorporation of these peptides into model membrane structures, e.g., DMPC vesicles, in aqueous buffer sometimes produces changes in the peptide secondary structure. Those peptides which possess a 3_{10}-helical structure in $CDCl_3$ solution change the secondary structure in DMPC vesicles to predominantly α-helical, plus a contribution from short, unstable 3_{10}-helix and/or β-turns. Those peptides which contain a combination of α- and 3_{10}-helical structures in $CDCl_3$ solution tend to retain some 3_{10}-helical structure within the lipid environment, although the overall H-bonding pattern is altered. Those peptides which form a β-bend ribbon structure appear to be largely unaffected in the membrane environment. This study represents the first complete characterization of a pure 3_{10}-helix and a pure β-bend ribbon by FTIR spectroscopy using resolution-enhancement techniques.

The secondary structure of membrane proteins and signal peptides present within a lipid matrix is of considerable interest at the present time. Some workers suggest that the α-helix is the dominant motif in these systems (Henderson et al., 1975; Deisenhofer et al., 1985; Austen, 1979; Briggs & Gierasch, 1984; Shinnar & Kaiser, 1984; Batenburg et al., 1988; Rosenblatt et al., 1980), whereas other workers suggest that appreciable amounts of β-sheet (Kleffel et al., 1985; Reddy & Nagaraj, 1989) or some 3_{10}-helical structure (Fox & Richards, 1982; Popot et al., 1990) may be present. Furthermore, the "helical hairpin hypothesis" of Engelman and Steitz (1981) supposes that the insertion of proteins into membranes is initiated by the spontaneous penetration of an α- or 3_{10}-helical hairpin from a hydrophobic portion of the protein into the bilayer.

Biophysical studies on transmembrane channels, such as those formed by peptides of the alamethicin family, suggest that both α- and 3_{10}-helical structures may occur (Mathew & Balaram, 1983; Menestrina et al., 1986). A recent survey of X-ray diffraction studies (Barlow & Thornton, 1988) has indicated that in addition to the α-helix, the 3_{10}-helical structure may also be present in various amounts in soluble proteins.

Various studies have shown that the α-aminoisobutyric acid (Aib)[1] residue promotes $\alpha/3_{10}$-helical structures (Prasad & Balaram, 1984; Toniolo & Benedetti, 1988; Toniolo, 1989; Smith et al., 1981). This unusual α-amino acid occurs extensively in the transmembrane channel forming peptaibol antibiotics (Benedetti et al., 1982a; Bruckner & Graf, 1983). Two of these polypeptides, alamethicin and trichorzianine, were found to be predominantly α-helical by X-ray diffraction analysis, but short segments of 3_{10}-helical were also observed (Fox & Richards, 1982; Le Bars et al., 1988).

Experimental evidence from electron diffraction photographs (Malcolm, 1983) and Raman and polarized IR absorption studies (Dwivedi et al., 1984) indicates that the 3_{10}-helix is the preferred conformation of polydisperse poly(Aib)$_n$. Dwivedi et al. (1984) calculate that the amide I band of poly(Aib)$_n$ in a 3_{10}-helical structure should absorb at 1665 cm^{-1}, while type III β-turns (a type III β-turn corresponds to the building unit of the 3_{10}-helix) should have amide I absorptions at 1686 and 1646 ± 3 cm^{-1}. A recent study of alamethicin by Haris and Chapman (1989) assigned the main peak at 1663 cm^{-1} to a combination of absorptions from 3_{10}- and α-helices, and suggested that the weaker band at 1639 cm^{-1} may also be associated with the 3_{10}-helical structure. ^1H NMR, IR absorption, and X-ray diffraction studies of terminally blocked, monodisperse (Aib)$_n$ (n = 2–10) homopeptides strongly support the formation of an intramolecular

† This work was supported by the SERC and the Wellcome Foundation.

‡ University of London.

§ University of Padua.

[1] Abbreviations; Z, benzyloxycarbonyl; *p*BrZ, *p*-bromobenzyloxycarbonyl; *p*BrBz, *p*-bromobenzoyl; Boc, *tert*-butoxycarbonyl; OMe, methoxy; O*t*Bu, *tert*-butoxy; Aib, α-aminoisobutyric acid; DMPC, dimyristoylphosphatidylcholine; pbs, phosphate-buffered saline; FTIR, Fourier transform infrared; NMR, nuclear magnetic resonance.

0006-2960/91/0430-6541$02.50/0

H-bonding pattern characteristic of the 3_{10}-helix occurring first at the trimer level (Benedetti et al., 1982b; Bavoso et al., 1986; Toniolo et al., 1985, 1986; Pavone et al., 1990).

X-ray diffraction studies of *p*BrBz-(Aib-L-Ala)$_{4,5}$-OMe crystallized from methanol have indicated that both peptides contain both α- and 3_{10}-helices under these conditions (Benedetti et al., 1990; Pavone et al., 1990).

Sequential oligomers containing the sequence Aib-L-Pro are also of interest as the presence of Pro in the sequence interrupts the H-bonding pattern. An NMR study by Venkatachalapathi and Balaram (1981) suggests that the peptide Z-(Aib-L-Pro)$_4$-OMe forms a type of 3_{10}-helix that has the alternating presence/absence of the intramolecular H-bond due to the alkylation of the amide group in the Pro residue. This structure is known as a β-bend ribbon and may be a conformational feature of some members of the alamethicin family, for example, zervamicin (Karle et al., 1987). The longest β-bend ribbon, so far fully characterized by X-ray diffraction analysis, is that formed by *p*BrBz-Aib-(L-Pro-Aib)$_4$-OMe (Toniolo et al., unpublished results).

FTIR spectroscopy is now an established technique for determining the secondary structure of proteins. The primary information on the polypeptide conformation is found in the amide I band. The IR absorption studies of terminally blocked (Aib)$_n$ peptides (Benedetti et al., 1982b; Toniolo et al., 1985) related the position of the amide I maximum to the secondary structures present. This band, however, is not a pure band and consists of several components, each of which can be associated with various secondary structures. Resolution-enhancement techniques such as second derivative and deconvolution can be used to identify the positions of the components of the amide I band, from which the secondary structures can be identified.

This paper describes studies of peptides which are known to exist as 3_{10}-helical structures, a combination of 3_{10}- and α-helices, or β-bend ribbon in $CDCl_3$ solution using FTIR spectroscopy combined with resolution-enhancement techniques. We ask the questions: (a) are there IR absorption bands which are characteristic, and can be used to indicate the presence of the 3_{10}-helical and the β-bend ribbon secondary structures, and (b) are the secondary structures which exist in solution modified when the peptides are incorporated into a model lipid biomembrane?

Materials and Methods

The synthesis and characterization of Z-(Aib)$_n$-O*t*Bu (n = 3–10) (Jones et al., 1965; Toniolo et al., 1985), Z-(Aib-L-Ala)$_n$-OMe (n = 2–5) and Z-L-Ala-(Aib-L-Ala)$_n$-OMe (n = 1–5) (Benedetti et al., 1990; Pavone et al., 1990), and *p*BrZ-(L-Pro-Aib)$_n$-OMe (n = 1–5) (Toniolo et al., unpublished results) have already been described.

$CDCl_3$ and DMPC were both purchased from Sigma Chemicals Ltd., England. Solution studies were carried out in $CDCl_3$ at 20, 40, and 50 °C.

The spectra in aqueous lipid dispersion were prepared by adding DMPC and the peptide to chloroform in a lipid:peptide ratio of 15:1. After the samples were dried under N_2 and then under vacuum, small volumes of phosphate-buffered saline, pH 7.4, were added, and the samples were incubated above the phase transition of the lipid for 2–3 h. This is similar to the method of Rizzo et al. (1987) for incorporating alamethicin into the lipid dispersion. Samples in D_2O buffer, pD 7.4, were incubated at 33 °C for 22–24 h in order to allow hydrogen–deuterium exchange to occur in the peptide.

Spectra were obtained with a Perkin-Elmer 1750 FTIR spectrometer equipped with a TGS detector and a Perkin-Elmer 7300 computer for data acquisition and analysis. Samples were placed in a thermostated Beckman FH-01 CFT microcell fitted with CaF_2 windows, and a 50-μm Teflon spacer was used for measurements of the 16 mM samples in $CDCl_3$ and a 0.6-mm Teflon spacer for 1.5 mM samples. For the aqueous solutions, a 6-μm tin spacer was used for samples in H_2O buffer, and a 50-μm Teflon spacer for samples in D_2O buffer. Temperature control was achieved by means of a cell jacket of circulating water. The spectrometer was continuously purged with dry air to eliminate water vapor absorptions from the spectral region of interest. A sample shuttle was used to permit the background to be signal-averaged concurrently with the sample.

Solvent spectra were recorded in a similar cell and under identical instrument conditions as the sample spectra. Difference spectra were obtained by digitally subtracting the solvent spectrum from the corresponding sample spectrum. Second-derivative (Moffat et al., 1986) and deconvolution using the Perkin-Elmer ENHANCE routine [analogous to the method of Kauppinen et al. (1981)] were used to assign features of the composite amide I band to structural features present in the peptide.

Table I: Components of the Resolution-Enhanced Amide I and Amide II Bands of Z-(Aib)$_n$-O*t*Bu (n = 3–10) at 1.5 mM Concentration in $CDCl_3$[a]

n	amide I (cm^{-1})	amide II (cm^{-1})
10	1681 w, 1662 s, 1646 w	1533 s
9	1681 w, 1663 s, 1644 w	1532 s, 1558 w
8	1679 w, 1666 s, 1646 w	1532 s
7	1680 w, 1670 s, 1648 w	1531 s, 1557 w
6	1677 s, 1664 w, 1649 w	1531 s, 1537 w
5	1680 s, 1668 w	1526 s, 1537 w
4	1682 s, 1662 w	1517 s, 1530 w
3	1687 s, 1664 w	1523 s, 1538 w

[a] s = strong, w = weak.

Results

Studies in Organic Solvent. The absorption spectra of the Z-(Aib)$_n$-O*t*Bu series (n = 3–10) at 1.5 mM concentration in $CDCl_3$ show the same pattern as that recorded by Toniolo et al. (1985). The position of the amide I band shows a decrease in the frequency as n increases. Similarly, the bands from the free urethane and peptide N–H groups at 3450–3400 cm^{-1} and the intramolecularly H-bonded N–H groups at 3380–3320 cm^{-1} behave as previously reported for the peptides in the absence of self-association.

Second-derivative and deconvolution techniques give further information about the structure within the amide I absorption. The frequencies of the main band and of minor components of the amide I band for the 1.5 mM solutions of Z-(Aib)$_n$-O*t*Bu (n = 3–10) in $CDCl_3$ are given in Table I. The absorption spectrum of Z-(Aib)$_8$-O*t*Bu in $CDCl_3$, with the deconvolved and second-derivative spectra of the same peptide, is shown in Figure 1 (a, b, and c, respectively).

For n = 8–10, the resolution-enhanced spectra of the amide I band show three components: the main absorption band, which occurs at 1666–1662 cm^{-1} and we assign to 3_{10}-helix, and two smaller components of approximately equal intensity, one at 1646–1644 cm^{-1}, which we assign to type III β-turns, and one at 1681–1679 cm^{-1}, which may be from type III β-turns and/or free carbonyl groups. The amide II band has one strong component, whose peak is centered at 1533–1532 cm^{-1}. The band at 1716–1715 cm^{-1}, corresponding to the overlapping absorptions of H-bonded urethane C=O and free *tert*-butyl ester C=O groups of the N- and C-protecting moieties (Pulla Rao et al., 1980; Bonora et al., 1984), cannot

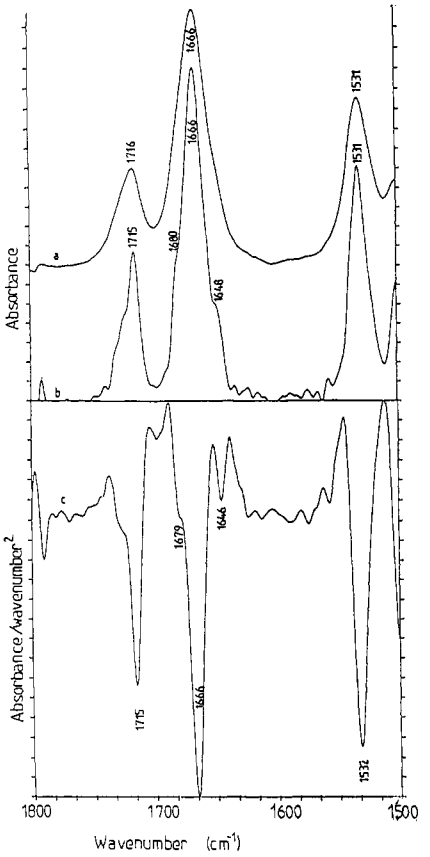

FIGURE 1: (a) FTIR absorption spectrum from 1800 to 1500 cm^{-1} of Z-(Aib)$_8$-O*t*Bu in $CDCl_3$ at 20 °C. (b) Deconvolved spectrum of Z-(Aib)$_8$-O*t*Bu in $CDCl_3$ at 20 °C using bandwidth 12 and resolution-enhancement factor 2.125. (c) Second-derivative spectrum of Z-(Aib)$_8$-O*t*Bu in $CDCl_3$ at 20 °C.

Table II: Components of the Resolution-Enhanced Amide I and Amide II Bands of Z-(Aib-L-Ala)$_n$-OMe (n = 1–5) at 1.5 mM Concentration in $CDCl_3$[a]

n	amide I (cm^{-1})	amide II (cm^{-1})
5	1681 w, 1662 s, 1659 s, 1649 w, 1641 w	1537 s
4	1673 w, 1664 s, 1644 w	1535 s
3	1673 s, 1657 w	1528 s
2	1681 s, 1664 w	1534 w, 1514 s
1	1677 s	1513 s

[a] s = strong, w = weak.

be separated by using resolution-enhancement techniques.

The results of the study of the Z-(Aib-L-Ala)$_n$-OMe (n = 1–5) peptides in $CDCl_3$ at 1.5 mM concentration are listed in Table II. The absorption spectrum of Z-(Aib-L-Ala)$_5$-OMe (Figure 2a) shows the amide I band at 1662 cm^{-1} and the amide II band at 1536 cm^{-1}. The deconvolved spectrum (Figure 2c) is able to resolve the main amide I absorption into two main components, one at 1662 cm^{-1}, assigned to 3_{10}-helix, and one at 1659 cm^{-1}, assigned to α-helix. The band identified at 1681 cm^{-1} is assigned to type III β-turns and/or free carbonyl groups. The bands at 1649 and 1641 cm^{-1} are either in or very close to the predicted frequency range for type III β-turns (Krimm & Bandekar, 1986). However, the $3\pi/2$ vibration of the α-helix may also absorb in this region (Lee et al., 1985), making definite assignment of the these bands difficult. The broad band centered around 1743 cm^{-1} should be related to the free methyl ester carbonyl group and the band centered at 1713 cm^{-1} to the H-bonded urethane carbonyl group. The second-derivative spectrum (Figure 3a) is unable to resolve the two major bands and shows one asymmetric main band at 1662 cm^{-1} which we assign to a combination of α- and

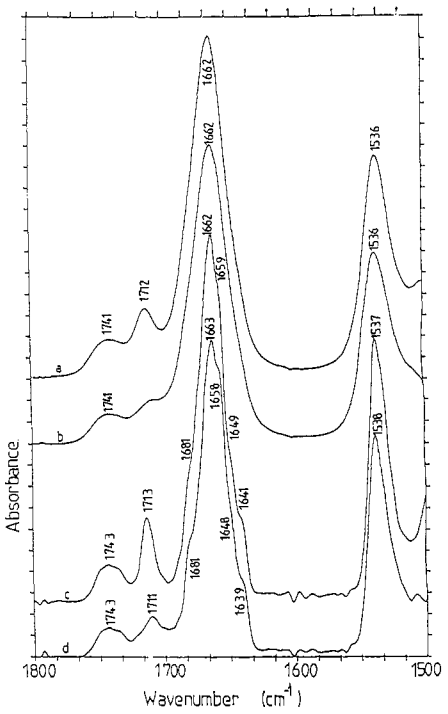

FIGURE 2: (a) FTIR absorption spectrum from 1800 to 1500 cm^{-1} of 1.5 mM Z-(Aib-L-Ala)$_5$-OMe in $CDCl_3$ at 20 °C. (b) FTIR absorption spectrum from 1800 to 1500 cm^{-1} of 1.5 mM Z-L-Ala-(Aib-L-Ala)$_5$-OMe in $CDCl_3$ at 20 °C. (c) Deconvolved spectrum of 1.5 mM Z-(Aib-L-Ala)$_5$-OMe in $CDCl_3$ at 20 °C using bandwidth 12 and resolution-enhancement factor 2.125. (d) Deconvolved spectrum of 1.5 mM Z-L-Ala-(Aib-L-Ala)$_5$-OMe in $CDCl_3$ at 20 °C using bandwidth 12 and resolution-enhancement factor 2.125.

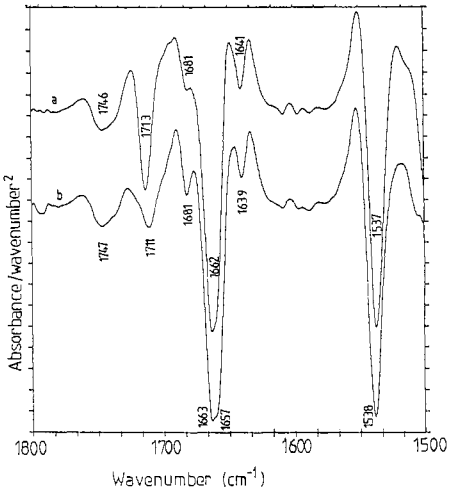

FIGURE 3: (a) Second-derivative spectrum of 1.5 mM Z-(Aib-L-Ala)$_5$-OMe in $CDCl_3$ at 20 °C. (b) Second-derivative spectrum of 1.5 mM Z-L-Ala-(Aib-L-Ala)$_5$-OMe in $CDCl_3$ at 20 °C.

Table III: Components of the Resolution-Enhanced Amide I and Amide II Bands of Z-L-Ala-(Aib-L-Ala)$_n$-OMe (n = 1–5) at 1.5 mM Concentration in $CDCl_3$[a]

n	amide I (cm^{-1})	amide II (cm^{-1})
5	1681 w, 1663 s, 1658 s, 1649 w, 1641 w	1538 s
4	1680 w, 1667 s, 1647 w	1533 s
3	1679 w, 1667 s, 1647 w	1533 s
2	1679 s, 1657 w	1533 w, 1514 s
1	1679 w, 1665 s	1507 w

[a] s = strong, w = weak.

3_{10}-helices. Two smaller side bands are also identified at 1641 and 1681 cm^{-1}, but the feature at 1649 cm^{-1} seen in the deconvolved spectrum is lost in the negative lobe of the main band.

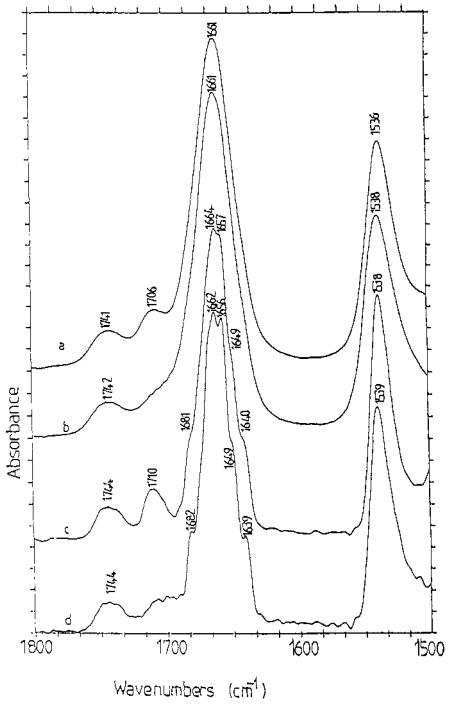

FIGURE 4: (a) Absorption spectrum of 16 mM Z-(Aib-L-Ala)$_5$-OMe in $CDCl_3$ at 20 °C. (b) Absorption spectrum of 16 mM Z-L-Ala-(Aib-L-Ala)$_5$-OMe in $CDCl_3$ at 20 °C. (c) Deconvolved spectrum of 16 mM Z-(Aib-L-Ala)$_5$-OMe in $CDCl_3$ at 20 °C using bandwidth 12 and resolution-enhancement factor 2.125. (d) Deconvolved spectrum of 16 mM Z-L-Ala-(Aib-L-Ala)$_5$-OMe in $CDCl_3$ at 20 °C using bandwidth 12 and resolution-enhancement factor 2.125.

Table IV: Components of the Resolution-Enhanced Amide I and Amide II Bands of *p*Brz-(L-Pro-Aib)$_n$-OMe (n = 2–5) at 1.5 mM concentration in $CDCl_3$[a]

n	amide I (cm^{-1})	amide II (cm^{-1})
5	1682 w, 1661 w, 1645 s	1538 s
4	1682 w, 1664 w, 1648 s, 1641 w	1538 s
3	1685 s, 1663 s, 1644 w	1537 s
2	1684 s, 1664 w	1536 s

[a] s = strong, w = weak.

The results of the study of the peptides Z-L-Ala-(Aib-L-Ala)$_n$-OMe (n = 1–5) in $CDCl_3$ at 1.5 mM concentration are listed in Table III. The absorption spectrum of Z-L-Ala-(Aib-L-Ala)$_5$-OMe (Figure 2b) shows the amide I band at 1662 cm^{-1} and the amide II band at 1536 cm^{-1}. The deconvolved and second-derivative spectra (Figures 2d and 3b, respectively) indicated that the main band is formed by two components, one at 1663 cm^{-1}, which we assign to 3_{10}-helix, and one at 1657–1658 cm^{-1}, which we assign to α-helix. Furthermore, the minor component at 1681 cm^{-1} we assign to type III β-turns and/or free carbonyl groups. The bands at 1639 and 1648 cm^{-1} may be from type III β-turns, with a possible contribution from the $3\pi/2$ vibration of the α-helix. There is also a band 1743–1747 cm^{-1} which we assign to the free methyl ester carbonyl group and one at 1711 cm^{-1}, assigned to the H-bonded urethane carbonyl group.

The absorption and resolution-enhanced spectra of Z-L-Ala-(Aib-L-Ala)$_5$-OMe and Z-(Aib-L-Ala)$_5$-OMe in $CDCl_3$ at 16 mM concentration show similar spectra when compared to those at the lower concentration, but better separation of the bands assigned to α- and 3_{10}-helices was achieved by using the same resolution-enhancement factors (Figures 4 and 5).

The results of the studies of the *p*BrZ-(L-Pro-Aib)$_n$-OMe (n = 2–5) peptides are given in Table IV. The absorption spectrum of *p*BrZ-(L-Pro-Aib)$_5$-OMe and the deconvolved and second-derivative spectra are shown in Figure 6a–c, respectively. The absorption spectrum shows two amide I components: the main feature at 1645 cm^{-1}, which we assign to a combination of H-bonded secondary amide and free tertiary amide carbonyls present in a β-bend ribbon, and a smaller component at 1680 cm^{-1}, which we assign to free carbonyl groups. The amide II band is seen at 1538 cm^{-1}. Resolution-enhancement techniques identify the position of the high-frequency component at 1682 cm^{-1} and resolved a further band at 1661–1658 cm^{-1}. The band at 1736 cm^{-1} is assigned to the free methyl ester carbonyl group.

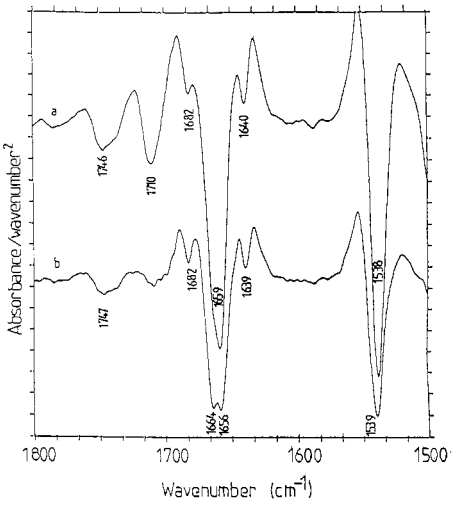

FIGURE 5: (a) Second-derivative spectrum of 16 mM Z-(Aib-L-Ala)$_5$-OMe in $CDCl_3$ at 20 °C. (b) Second-derivative spectrum of 16 mM Z-L-Ala-(Aib-L-Ala)$_5$-OMe in $CDCl_3$ at 20 °C.

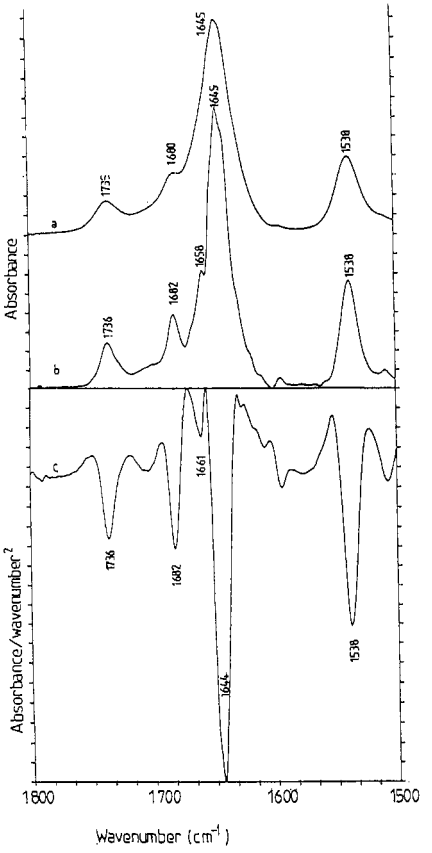

FIGURE 6: (a) FTIR absorption spectrum from 1800 to 1500 cm^{-1} of *p*BrZ-(L-Pro-Aib)$_5$-OMe in $CDCl_3$ at 20 °C. (b) Deconvolved spectrum of *p*BrZ-(L-Pro-Aib)$_5$-OMe using bandwidth 12 and resolution-enhancement factor 2.125. (c) Second-derivative spectrum of *p*BrZ-(L-Pro-Aib)$_5$-OMe in $CDCl_3$ at 20 °C.

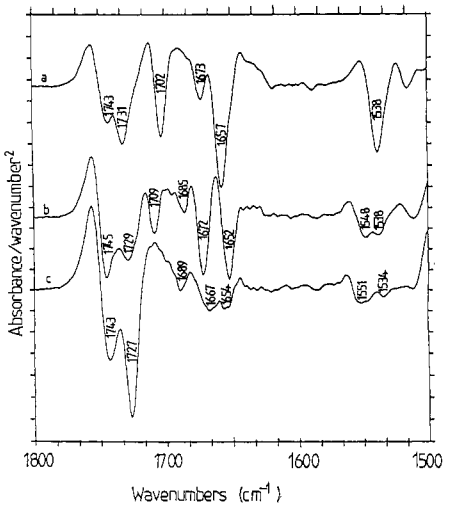

FIGURE 7: (a) Second-derivative spectrum of Z-(Aib)$_8$-O*t*Bu in DMPC vesicles (approximate molar ratio 1:15) in pbs buffer, pH 7.4. (b) Second-derivative spectrum of Z-(Aib-L-Ala)$_5$-OMe in DMPC vesicles (approximate molar ratio 1:15) in pbs buffer, pH 7.4. (c) Second-derivative spectrum of Z-L-Ala-(Aib-L-Ala)$_5$-OMe in DMPC vesicles (approximate molar ratio 1:15) in pbs buffer, pH 7.4.

Studies of Peptides in Aqueous Lipid Dispersion. The influence of lipids on the secondary structure of the peptides was investigated by using DMPC vesicles. Figure 7a shows the second-derivative spectrum of Z-(Aib)$_8$-O*t*Bu in DMPC vesicles at 30 °C (above T_c). We assign the bands at 1743 and 1731 cm^{-1} to the lipid ester groups. The amide I band of the peptide exhibits two components: one at 1657 cm^{-1}, characteristic of α-helix, and the other at 1673 cm^{-1}, characteristic of short, unstable 3_{10}-helix and/or β-turns. We assign the band at 1702 cm^{-1} to the H-bonded urethane carbonyl group and the *tert*-butyl ester carbonyl group. The frequencies of the amide I and II bands are unchanged at 20 °C (below the lipid transition temperature). Similar results are obtained for Z-(Aib)$_n$-O*t*Bu (n = 9, 10). The experiment was repeated in D_2O buffer, using Z-(Aib)$_8$-O*t*Bu in DMPC vesicles. The second-derivative spectrum is shown in Figure 8a. The spectrum is very similar to that of the sample in H_2O buffer and shows that, despite the long incubation in the D_2O buffer, little, if any, H ↔ D exchange occurs. Similar results were obtained for Z-(Aib)$_n$-O*t*Bu (n = 9, 10).

The second-derivative spectrum of Z-(Aib-L-Ala)$_5$-OMe reconstituted in DMPC vesicles (Figure 7b) shows two main components at 1652 cm^{-1}, assigned to α-helix, and at 1672 cm^{-1}, which we assign to a short, unstable 3_{10}-helix and/or β-turns. The small band at 1685 cm^{-1} is assigned to β-turns. The sharp band at 1709 cm^{-1} is assigned to the H-bonded urethane carbonyl of the N-protecting group, and it is noted that the intensity of this band is greatly increased relative to the intensity in $CDCl_3$. Incubation of the sample in D_2O buffer induced a large shift in the amide II band, indicating a high level of H ↔ D exchange. The second-derivative spectrum (Figure 8b) has components at 1677 cm^{-1}, which we assign to β-turns, 1661 cm^{-1}, assigned to exchanged 3_{10}-helix, and 1642 cm^{-1}, which we assign to α-helix (see Discussion).

The second-derivative spectrum of Z-L-Ala-(Aib-L-Ala)$_5$-OMe in DMPC vesicles (Figure 7c) shows the main components of the amide I band at 1667 cm^{-1}, assigned to 3_{10}-helix, and 1654 cm^{-1}, assigned to α-helix. The intensity of the amide I absorption in this spectrum is relatively weak, and we were unable to improve on this result when repeating the experiment. Incubation of Z-L-Ala-(Aib-L-Ala)$_5$-OMe incorporated in DMPC vesicles in D_2O buffer caused the disappearance of the amide II band, indicating a high level of H ↔ D exchange. The second-derivative spectrum (Figure 8c) shows the major amide I component at 1659 cm^{-1}. This is too high to be deuterated α-helix, and therefore we assign the band to deuterated 3_{10}-helix, possibly with a contribution from α-helix.

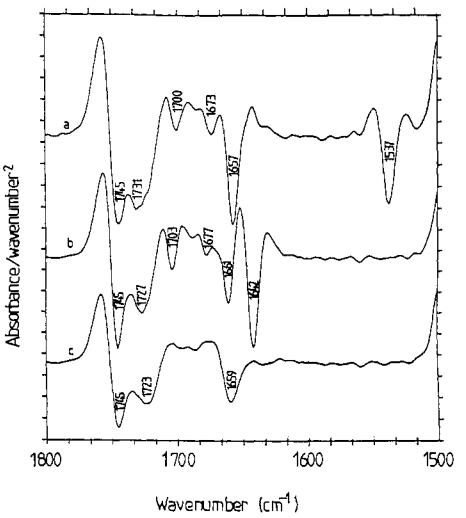

FIGURE 8: (a) Second-derivative of Z-(Aib)$_8$-O*t*Bu in DMPC vesicles (approximate molar ratio 1:15) in pbs buffer, pD 7.4, after incubation at 33 °C for 22–24 h. (b) Second-derivative spectrum of Z-(Aib-L-Ala)$_5$-OMe in DMPC vesicles (approximate molar ratio 1:15) in pbs buffer, pD 7.4, after incubation at 33 °C for 22–24 h. (c) Second-derivative spectrum of Z-L-Ala-(Aib-L-Ala)$_5$-OMe in DMPC vesicles (approximate molar ratio 1:15) in pbs buffer, pD 7.4, after incubation at 33 °C for 22–24 h.

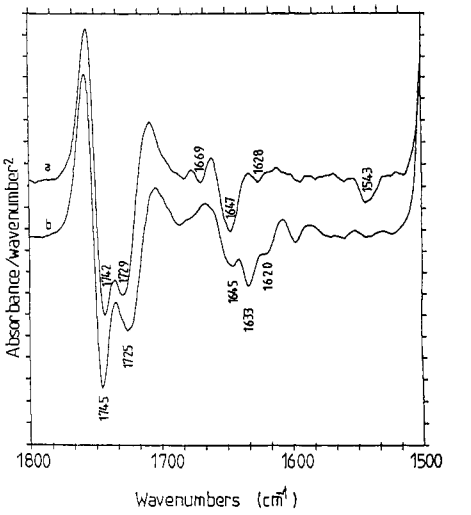

FIGURE 9: (a) Second-derivative spectrum of *p*BrZ-(L-Pro-Aib)$_5$OMe in DMPC vesicles (approximate molar ratio 1:15) in pbs buffer, pH 7.4. (b) Second-derivative spectrum of *p*BrZ-(L-Pro-Aib)$_5$-OMe in DMPC vesicles in pbs buffer, pD 7.4, after incubation at 33 °C for 22–24 h.

The second-derivative spectrum of *p*BrZ-(L-Pro-Aib)$_5$-OMe reconstituted in DMPC vesicles (Figure 9a) gives the main amide I component at 1647 cm^{-1}, assigned to β-bend ribbon, with smaller components at 1669 and 1628 cm^{-1}, both assigned to β-turns. The use of D_2O buffer causes H ↔ D exchange in the peptide, and the second-derivative spectrum (Figure 9b) shows three amide I components: 1633 cm^{-1}, assigned to exchanged β-bend ribbon; 1645 cm^{-1}, assigned to unexchanged β-bend ribbon; and 1620 cm^{-1}, assigned to β-turns.

Discussion

The $C^{\alpha,\alpha}$-dialkylated α-amino acid Aib has been shown to promote formation of helical conformations (Smith et al., 1981;

Prasad & Balaram, 1984; Toniolo, 1989; Toniolo & Benedetti, 1988). Conformation energy calculations, assuming a tetrahedral symmetric geometry for the four substituents on the C^{α} carbon, predicted that an α-helical structure would be adopted by the Aib residue (Marshall, 1971; Pletnev et al., 1973; Burgess & Leach, 1973). However, the assumption of symmetry has been shown to be invalid for crystallized peptides containing poly(Aib)$_n$. For a residue in a right-handed (incipient) 3_{10}-helical conformation, the bond angles involving the methyl group in the D-position tend to be larger than the tetrahedral value, whereas those involving the L-methyl group tend to be smaller. This slight distortion is due to steric hindrance as the formation of the 3_{10}-helix involves the methyl in the D-position being too close to the C=O of the preceding unit. Taking this asymmetry into account, Paterson et al. (1981) showed that the 3_{10}-helix is the most stable conformation for Aib homopeptides.

A number of conformational studies on terminally blocked Aib-containing peptides have been carried out by using a range of techniques, including X-ray diffraction as well as ^{1}H and ^{13}C NMR and IR absorption spectroscopy. A ^{13}C NMR study of Z-(Aib)$_n$-OMe (n = 3–8) by Saitô et al. (1988) showed that all these homopeptides contain incipient or fully developed 3_{10}-helices. Toniolo et al. (1985, 1986) conclude from studies using X-ray diffraction and IR absorption spectroscopy that fully stable 3_{10}-helices are formed by Z-(Aib)$_n$-O*t*Bu for n = 8 or more.

Recent papers by Karle, Balaram, and co-workers on Aib-rich peptides show that the peptide Boc-Trp-Ile-Ala-Aib-Ile-Val-Aib-Leu-Aib-Pro-OMe exhibits a predominantly α-helical structure in triclinic crystals and a 3_{10}-helix in monoclinic crystals (Karle et al., 1989a). The same workers also reported that two molecules of the peptide Boc-Aib-Val-Aib-Aib-Val-Val-Val-Aib-Val-Aib-OMe cocrystallize in a triclinic cell with different helical conformations (Karle et al., 1989a), one molecule being totally α-helical and the other being a combination of α-helix and 3_{10}-helix. Solution studies using ^{1}H NMR on the same compound found it to be completely 3_{10}-helical in $CDCl_3$ and either α-helical or partially unfolded 3_{10}-helical in $(CD_3)_2SO$. Studies in $CDCl_3$ are widely carried out as this solvent has a low polarity, similar to the low polarity experienced in natural membranes.

Bavoso et al. (1988) summarized the current empirical view based on X-ray data that, while Aib-rich peptides shorter than eight residues tend to adopt a 3_{10}-helical structure, Aib-rich peptides of eight residues or longer may adopt either 3_{10}- or mixed $3_{10}/\alpha$-helical structure.

Marshall et al. (1990) concluded that the choice between the α- and 3_{10}-helical conformations assumed by peptides containing multiple $C^{\alpha,\alpha}$-dialkylated amino acids depends on peptide length, environment, and size and distribution of amino acid side chains.

The interpretation of the 1750–1600 cm^{-1} region of the IR absorption spectrum for these peptides is complicated by the presence of free peptide carbonyl groups and by the N- and C-terminal protecting groups. The urethane C=O of the benzyloxycarbonyl protecting group is the acceptor of the first H-bond. A free urethane C=O occurs at a frequency >1725 cm^{-1}, whereas the band from a H-bonded urethane C=O occurs at 1720–1715 cm^{-1} (Pulla Rao et al., 1980; Bonora et al., 1984). However, the carbonyl of the *tert*-butyl ester group also occurs at 1720–1715 cm^{-1}, while the band from the carbonyl of the methyl ester group occurs at 1740–1730 cm^{-1}.

In all the 3_{10}-helical peptides examined in the present study, the last two carbonyl groups are not H-bonded. As the number of Aib residues decreases, the absorption of the free peptide carbonyls become relatively stronger with respect to that of the H-bonded peptide carbonyls. From Table I, as n decreases, the relative increase in intensity of the band centered around 1687–1677 cm^{-1} indicates that this band arises from free peptide carbonyls. The increase in intensity of the band in the range 1666–1662 cm^{-1} as n increases indicates that this is due to H-bonded peptide carbonyls. This frequency range, coupled with the position of the amide II at 1533–1531 cm^{-1}, agrees well with the calculated frequencies of Krimm and Bandekar (1980) for the 3_{10}-helical structure.

The two minor components of the amide I band for the Z-(Aib)$_n$-O*t*Bu (n = 8–10) homopeptides occur at 1681–1679 and 1646–1644 cm^{-1}. These components remain after the sample has been diluted to a concentration approximately 4 times below the minimum level for self-aggregation, indicating that they derive from secondary structures present in the monomeric peptides. The observed frequencies agree well with the predicted values of 1686 and 1646 ± 3 cm^{-1} for type III β-turn absorptions. Therefore, we assign the band at 1646–1644 cm^{-1} to type III β-turns and the band at 1681 cm^{-1} to type III β-turns and/or free carbonyls.

The resolution-enhanced spectra of the Z-(Aib-L-Ala)$_n$-OMe and Z-L-Ala-(Aib-L-Ala)$_n$-OMe peptides in $CDCl_3$ indicate that in both peptide series the highest oligomers contain a combination of α- and 3_{10}-helix.

We interpret the spectral shift observed with the Z-(Aib)$_n$-O*t*Bu (n = 8–10) peptides using DMPC vesicles to indicate that the peptides shift from a 3_{10}-helical conformation in $CDCl_3$ to mainly α-helical, with a contribution from β-turns and/or short, unstable 3_{10}-helix, in aqueous lipid dispersion. No further change in the peptide secondary structure is detected upon raising the temperature from below to above the phase transition temperature of the lipid. Karle et al. (1988, 1989a) have shown that two different conformations are possible for the same peptide in its crystalline form, illustrating the sensitivity of the peptide secondary structure to its particular environment.

The inability of the peptide to undergo H ↔ D exchange when incorporated in DMPC vesicles indicates the inaccessibility of the peptide to D_2O molecules in this environment.

We interpret the spectral changes observed when the peptide Z-(Aib-L-Ala)$_5$-OMe is incorporated into an aqueous lipid dispersion to indicate that 3_{10}- and α-helical structures are still present. The frequencies of the 1652 and 1642 cm^{-1} bands assigned to α-helix in the undeuterated and deuterated peptide, respectively, are both low for regular α-helices. Karle et al. (1989b,c) reported the insertion of water molecules into the helical backbone of the apolar peptides Boc-Ala-Leu-Aib-Ala-Leu-Aib-OMe (Karle et al., 1989b) and Boc-Aib-(Val-Ala-Leu-Aib)$_3$-OMe (Karle et al., 1989c) when each was crystallized individually. In the first example, H-bonds are formed between the water and the C=O and NH groups of the Ala residues. This causes a bend in the backbone of the peptide and also increases the length of at least one of the intramolecular H-bonds, and may give rise to the low-frequency amide I components of the α-helical structure. This is similar to the low-frequency amide I′ band component assigned to the highly solvated α-helical structure observed for troponin C (Jackson et al., unpublished results), in which the intramolecular H-bonding pattern of the B-helix is interrupted by approximately 20% of the C=O groups H-bonding to water molecules inserted into the helical backbone.

An increase in the intensity of the band assigned to the H-bonded urethane carbonyl group may indicate intermole-

cular H-bonding of this group in the peptide aggregate in the lipid environment, or possibly indicate H-bonding to the lipid head-group.

The H ↔ D exhange of Z-(Aib-L-Ala)$_5$-OMe and Z-L-Ala-(Aib-L-Ala)$_5$-OMe when incorporated in lipid vesicles indicates that in this environment the hydrogen atoms of the amide NH groups are easily accessible to D_2O molecules. This indicates that the peptides aggregate to form pores in the bilayer which allows the passage of water molecules.

The components of the amide I band of Z-L-Ala-(Aib-L-Ala)$_5$-OMe incorporated in DMPC vesicles in H_2O show bands at 1667 and 1654 cm^{-1}, assigned to 3_{10}-helix and to α-helix, respectively. In D_2O, the same peptide shows a dominant feature at 1659 cm^{-1}, which we assign to deuterated 3_{10}-helix with perhaps a contribution from α-helix.

The NMR and IR absorption spectroscopy results for Z-(Aib-L-Pro)$_4$-OMe (Venkatachalapathi et al., 1981) indicate that the H-bonds formed may be slightly different from those of an ideal 3_{10}-helix due to the steric hindrance introduced by the presence of Pro residues. Unfavorable steric contacts required for an ideal 3_{10}-helix may be relaxed in this peptide by slight distortions introduced by nonplanar peptide units and deviations from the ideal 3_{10}-helical angles. These effects may alter the strength of the intramolecular H-bonds to produce the amide I absorption maximum at 1648–1645 cm^{-1} for *p*BrZ-(L-Pro-Aib)$_5$-OMe, which we assign to β-bend ribbon.

Incorporation of this peptide into DMPC vesicles produces very little effect on the amide I and II bands. The increased steric hindrance of the Pro-Aib peptides will reduce the number of possible conformations available and will require large pertrubations to induce change. However, the peptide *p*BrZ-(L-Pro-Aib)$_5$-OMe does undergo H ↔ D exchange when incorporated into DMPC vesicles in D_2O buffer, indicating that a pore may be formed by aggregates of the peptide within the lipid bilayer.

This study represents the first characterization of the 3_{10}-helical and β-bend ribbon secondary structures of FTIR spectroscopy incorporating resolution-enhancement techniques. We have shown that the main absorption from the stable 3_{10}-helix occurs at 1666–1662 cm^{-1} and from the β-bend ribbon at 1648–1645 cm^{-1}. We also demonstrate that with resolution-enhancement techniques it can be possible to identify α- and 3_{10}-helices in the same peptide.

These reults indicate that Aib homopeptides have a 3_{10}-helical secondary structure in $CDCl_3$ and are predominantly α-helical when incorporated into lipid vesicles. Peptides with Aib-L-Ala as the repeat unit tend to retain some of the 3_{10}-helical structure that they exhibit in $CDCl_3$ when incorporated into an aqueous model membrane. Further, we have shown that the 3_{10}-helical structure is very sensitive to changes in environment.

Registry No. DMPC, 18194-24-6; Z-(Aib)8-OBu-t, 95842-05-0; Z-(Aib-L-Ala)5-OMe, 133850-20-1; Z-L-Ala-(Aib-L-Ala)5-OMe, 131738-94-8; *p*-Brz-(L-Pro-Aib)5-OMe, 133833-18-8.

References

Austen, B. M. (1979) *FEBS Lett. 103*, 308–313.

Barlow, D. J., & Thornton, J. M. (1988) *J. Mol. Biol. 201*, 601–619.

Batenburg, A. M., Brasseur, R., Ruysschaert, J. M., van Scharrenburg, G. J. M., Slotboom, A. J., Demel, R. A., & de Kruijff, B. (1988) *J. Biol. Chem. 263*, 4202–4207.

Bavoso, A., Benedetti, E., Di Blasio, B., Pavone, C., Toniolo, C., & Bonora, G. M. (1986) *Proc. Natl. Acad. Sci. U.S.A. 83*, 1988–1992.

Bavoso, A., Benedetti, E., Di Blasio, B., Pavone, V., Pedone, C., Toniolo, C., Bonora, G. M., Formaggio, F., & Crisma, M. (1988) *J. Biomol. Struct. Dyn. 5*, 803–817.

Benedetti, E., Bavoso, A., Di Blasio, B., Pavone, V., Pedone, C., Toniolo, C., & Bonora, G. M. (1982a) *Proc. Natl. Acad. Sci. U.S.A. 79*, 7951–7954.

Benedetti, E., Bavoso, A., Di Blasio, B., Pavone, V., Pedone, C., Crimsa, M., Bonora, G. M. & Toniolo, C. (1982b) *J. Am. Chem. Soc. 104*, 2437–2444.

Benedetti, E., Di Blasio, B., Pavone, V., Pedone, C., Santini, A., Bavoso, A., Toniolo, C., Crisma, M., & Sartore, L. (1990) *J. Chem. Soc., Perkin Trans. 2*, 1829–1837.

Bonora, G. M., Mappeli, C., Toniolo, C., Wilkening, R. R., & Stevens, E. S. (1984) *Int. J. Biol. Macromol. 6*, 179–188.

Briggs, M. S., & Gierasch, L. M. (1984) *Biochemistry 23*, 3111–3114.

Bruckner, H., & Graf, H. (1983) *Experientia 39*, 528–530.

Burgess, A. W., & Leach, S. J. (1973) *Biopolymers 12*, 2599–2605.

Deisenhofer, J., Epp, O., Miki, K., Huber, R., & Michel, H. (1985) *Nature (London) 318*, 618–624.

Dwivedi, A. M., Krimm, S., & Malcolm, B. R. (1984) *Biopolymers 23*, 2025–2065.

Engelman, D. E., & Steitz, T. A. (1981) *Cell 23*, 411–422.

Fox, R., & Richards, F. M. (1982) *Nature (London) 300*, 325–330.

Haris, P. I., & Chapman, D. (1988) *Biochim. Biophys. Acta 943*, 375–380.

Henderson, R. (1975) *J. Mol. Biol. 93*, 123–138.

Jones, D. S., Kenner, G. W., Preston, J., & Sheppard, R. C. (1965) *J. Chem. Soc.*, 6227–6239.

Karle, I. L., Flippen-Anderson, J. L., Sukumar, M., & Balaram, P. (1987) *Proc. Natl. Acad. Sci. U.S.A. 84*, 5087–5091.

Karle, I. L., Flippen-Anderson, J. L., Sukumar, M., & Balaram, P. (1988) *Int. J. Pept. Protein Res. 31*, 567–576.

Karle, I. L., Flippen-Anderson, J. L., Uma, K., Balaram, H., & Balaram, P. (1989a) *Proc. Natl. Acad. Sci. U.S.A. 86*, 765–769.

Karle, I. L., Flippen-Anderson, J. L., Uma, K., & Balaram, P. (1989b) *Biopolymers 28*, 773–781.

Karle, I. L., Flippen-Anderson, J. L., Uma, K., & Balaram, P. (1989c) *Biochemistry 28*, 6696–6701.

Kauppinen, J. K., Moffat, D. J., Mantsch, H. H., & Cameron, D. G. (1981) *Appl. Spectrosc. 35*, 271–275.

Kleffel, B., Garavito, R. M., Baumeister, W., & Rosenbusch, J. P. (1985) *EMBO J. 4*, 1589–1592.

Krimm, S., & Bandekar, J. (1980) *Biopolymers 19*, 1–29.

Le Bars, M., Bachet, B., & Mornon, J. P. (1988) *Z. Kristallogr. 185*, 588.

Lee, D. C., Hayward, J. A., Restall, C. J., & Chapman, D. (1985) *Biochemistry 24*, 4364–4373.

Malcolm, B. R. (1983) *Biopolymers 22*, 319–322.

Marshall, G. R. (1971) in *Intra-Science Chemistry Reports* (Kharasch, N., Ed.) pp 305–316, Gordon and Breach, New York.

Marshall, G. R., Hodgkin, E. E., Langs, D. A., Smith, G. D., Zabrocki, J., & Leplawy, M. T. (1990) *Proc. Natl. Acad. Sci. U.S.A. 87*, 487–491.

Mathew, M. K., & Balaram, P. (1983) *Mol. Cell. Biochem. 50*, 47–64.

Menestrina, G., Voges, K. P., Jung, G., & Boheim, G. (1986) *J. Membr. Biol. 93*, 111–132.

Moffat, D. J., Kauppinen, J. K., Cameron, D. G., Mantsch, H. H., & Jones, R. N. (1986) *Computer programs for*

infrared spectrophometry, N.R.C.C. Bulletin No. 18, Ottawa, Canada.
Paterson, Y., Rumsey, S. M., Benedetti, E., Nemethy, G., & Sheraga, H. A. (1981) *J. Am. Chem. Soc. 103*, 2947-2955.
Pavone, V., Di Blasio, B., Santini, A., Benedetti, E., Pedone, C., Toniolo, C., & Crisma, M. (1990) *J. Mol. Biol. 214*, 633-635.
Pavone, V., Benedetti, E., Di Blasio, B., Pedone, C., Santini, A., Bavoso, A., Toniolo, C., Crisma, M., & Sartore, L. (1990) *J. Biomol. Struct. Dyn. 7*, 1321-1331.
Pletnev, V. Z., Gromov, E. P., & Popov, E. M. (1973) *Khim. Prir. Soedin. 9*, 224-229.
Popot, J. L., Engelman, D. M., Gurel, O., & Zaccai, G. (1990) *J. Mol. Biol. 210*, 829-847.
Prasad, B. V. V., & Balaram, P. (1984) *CRC Crit. Rev. Biochem. 16*, 307-348.
Pulla Rao, C., Nagaraj, R., Rao, C. N. R., & Balaram, P. (1980) *Biochemistry 19*, 425-431.
Reddy, G. L., & Nagaraj, R. (1989) *J. Biol. Chem. 264*, 16591-16597.
Rizzo, V., Stankowski, S., & Schwarz, G. (1987) *Biochemistry 26*, 2751-2759.
Rosenblatt, M., Beaudette, N. V., & Fasman, G. D. (1980) *Proc. Natl. Acad. Sci. U.S.A. 77*, 3983-3987.
Saitô, H., Tabeta, R., Formaggio, F., Crisma, M., & Toniolo, C. (1988) *Biopolymers 27*, 1607-1617.
Shinnar, A. E., & Kaiser, E. T. (1984) *J. Am. Chem. Soc. 106*, 5006-5007.
Smith, G. D., Pletnev, V. Z., Duax, W. L., Balasabramanian, T. M., Bosshard, H. E., Czerwinski, E. W., Kendrick, N. E., Matthews, F. S., & Marshall, G. R. (1981) *J. Am. Chem. Soc. 103*, 1493-1501.
Toniolo, C. (1989) *Biopolymers 28*, 247-257.
Toniolo, C., & Benedetti, E. (1988) *ISI Atlas Sci.: Biochem. 1*, 225-230.
Toniolo, C., Bonora, G. M., Barone, V., Bavoso, A., Benedetti, E., Di Blasio, B., Grimaldi, P., Lelj, F., Pavone, V., & Pedone, C. (1985) *Macromolecules 18*, 895-902.
Toniolo, C., Bonora, G. M., Bavoso, A., Benedetti, E., Di Blasio, B., Pavone, V., & Pedone, C. (1986) *Macromolecules 19*, 472-479.
Venkatachalapathi, Y. V., & Balaram, P. (1981) *Biopolymers 20*, 1137-1145.

Fourier Transform Infrared Study of the N Intermediate of Bacteriorhodopsin†

Jean-Marc Pfefferlé,‡ Akio Maeda,* Jun Sasaki, and Tôru Yoshizawa§
Department of Biophysics, Faculty of Science, Kyoto University, Kyoto 606, Japan
Received January 3, 1991; Revised Manuscript Received April 2, 1991

ABSTRACT: Visible absorption spectroscopic experiments show that the N intermediate is the main photoproduct of a highly hydrated film of the light-adapted bacteriorhodopsin (70% water by weight) at pH 10 and 274 K. The difference Fourier transform infrared spectrum between the N intermediate and unphotolyzed light-adapted bacteriorhodopsin was recorded under these conditions. A small amount of the M intermediate present did not affect this spectrum significantly. The difference spectrum exhibited a positive band at 1755 cm^{-1} (probably due to Asp-85) and a negative band at 1742 cm^{-1} (due to Asp-96), neither of which was observed for the M intermediate. The spectrum of the N intermediate at pH 7 was nearly identical with that at pH 10. Spectra at pH 10 also were measured with isotope-substituted samples. A vibrational band at 1692 cm^{-1} due to the peptide bond disappeared, and a band at 1558 cm^{-1} emerged upon formation of the N intermediate. The spectrum also displayed bands containing the N-H and C_{15}-H in-plane bending vibrational modes at 1394 and 1303 cm^{-1}. These frequencies are similar to those of the L intermediate while the intensities of these bands are larger than those in the L intermediate, suggesting that the Schiff bases of both the L and N intermediates have a strong hydrogen-bonding interaction with the protein and that the C_{12}-H to C_{15}-H region of the chromophore is less twisted in the N intermediate than in the L intermediate.

Bacteriorhodopsin in the purple membrane (bR)[1] is one of the retinoid proteins produced by *Halobacterium halobium* (Stoeckenius et al., 1979; Stoeckenius & Bogomolni, 1982). Its chromophore is retinal, linked to the protein moiety through the lysine-216 residue as a protonated Schiff base. Upon absorption of light by the chromophore, bR acts as a light-driven proton pump, by ejecting protons from the cell and taking up protons from the opposite side of the membrane. Asp-85 and -96, buried in the membrane, have been shown to be essential for these processes (Mogi et al., 1988), Asp-85 for the proton release step (Otto et al., 1990) and Asp-96 for the proton uptake step (Holz et al., 1989).

Resonance Raman experiments by Maeda et al. (1986) have revealed a photoproduct, L′, which is more stable at alkaline pH. By means of visible absorption spectroscopy, Drachev et al. (1987), Dancshazy et al. (1988), and Kouyama et al. (1988)

† This work was supported in part by Grants-in-Aid for Specially Promoted Research from the Japanese Ministry of Education, Science and Culture (63065002), by a research grant from the Human Frontier Science Program, and by the Joint Studies Program of the Graduate University for Advance Studies. J.-M.P. was supported by an exchange program between the Japan Society for the Promotion of Science and the Swiss National Science Foundation.
* Address correspondence to this author at the Department of Biophysics, Faculty of Science, Kyoto University, Kitashirakawa-Oiwakecho, Sakyo-ku, Kyoto 606, Japan.
‡ Present address: KU 4.39, Ciba-Geigy, 1870 Monthey, Switzerland.
§ Present address: Department of Applied Physics and Chemistry, The University of Electro-Communication, 1-5-1 Chofugaoka, Chofu, Tokyo 182, Japan.

[1] Abbreviations: bR, bacteriorhodopsin; FT-IR, Fourier transform infrared; BR^L, light-adapted bacteriorhodopsin; λ_{max}, wavelength of maximum absorption.

0006-2960/91/0430-6548$02.50/0